Asian Journal of Chemistry; Vol. 26, No. 15 (2014), 4819-4826

ASIAN JOURNAL OF CHEMISTRY

http://dx.doi.org/10.14233/ajchem.2014.16241

Synthesis, Characterization and Photophysical Properties of Graphene-Phthalocyanine Hybrid

FAN ZHANG[1,2,*], RUILIN MAN[1], ZHIYUAN PENG[1,2] and ZHIBO LIU[3]

[1]College of Chemistry and Chemical Engineering, Central South University, Changsha 410083, P.R. China
[2]College of Chemistry and Chemical Engineering, Jishou University, Jishou 416000, P.R. China
[3]Key Laboratory of Weak Light Non-linear Photonics, Ministry of Education and Teda Applied Physics School, Nankai University, Tianjin 300457, P.R. China

*Corresponding author: E-mail: zhangfan8346@sina.com

Received: 24 August 2013; *Accepted*: 9 October 2013; *Published online*: 16 July 2014; AJC-15579

The functionalization of reduced graphene oxide by phenyl carboxylic diazonium salt and the subsequent attachment of a symmetrically substituted Zn-phthalocyanine *via* amide reaction were described. The graphene derivative was characterized by Raman spectra, Ultraviolet/visible spectra, Fourier transform infrared spectra, thermogravimetric analysis, scanning electron microscope, transmission electron microscopy, atomic force microscopy, fluorescence emission spectra and Z-scan experiments. The nanocomposite exhibited excellent thermal performance, a strong quenching and stronger nonlinear optical performance than that of each individual and the mixture in nanosecond regime. The thermogravimetric analysis tests showed the high grafting efficiency of phthalocyanine to graphene. And the efficient fluorescence quenching and optical limiting properties of the hybrid demonstrated the possible photoinduced electron transfer or energy transfer mechanism between graphene and phthalocyanine.

Keywords: Phthalocyanine, Graphene, Z-scan, Functionalization.

INTRODUCTION

The outstanding properties of graphene-based materials have attracted substantial endeavors of implementing them into practical applications such as field-effect transistors[1,2], sensors[3,4], energy-storage[5,6], supercapacitors[7,8], solar cell, *etc*.[9]. Among them, solar energy conversion or electronic application devices constructed by photo- and electro-active building blocks using graphene or reduced graphene oxide constitute a hot topic[10,11]. To date, chemical fabrication of graphene has been focused on taking advantage of the superior properties of both graphene and the functionalized material. Graphene, as excellent electron acceptor just like carbon nanotubes and fullerene, can be functionalized with electron donors as donor-acceptor conjugates[12], photoelectron chemical cell[13], nonlinear optical material[14,15], *etc*. The combination of graphene and electron donors such as porphyrin[13,15], perylene-dicarboximide[16] and phthalocyanine1[2,17-22] have led to new materials giving photoexcitation to electron transfer processes. Among the wide variety of electron donor moieties, phthalocyanines, as planar, electron-rich, aromatic materials, characterized by remarkably high extinction coefficients in the visible region, have been widely used as chromophores to decorate carbon nanotubes[23-25], fullerene[26] and nano-onions[27] for the development of artificial photosynthetic devices and photoelectron cell. Therefore, the combination of graphene and phthalocyanines could result new materials with excellent photoelectric properties[12,17-22]. However, a few reports devoted to fabricating graphene/phthalocyanines hybrid for nonlinear optical (NLO) properties research. Zhu *et al.*[17] reported that graphene oxide (GO) functionalized with unsymmetrically substituted zinc phthalocyanine for broad-band optical limiting. But the photo- and electro-properties of graphene-based phthalocyanines remain largely unexplored.

The presences of epoxy, hydroxyl and carboxylic groups on the base plane of GO resulted in the structure defect and a conversion from metallic to an insulator[28,29] and these functional groups provided a platform for the modification of GO. The structure and electronic properties defects of reduced graphene oxide were repaired compared with GO because the oxygen-containing groups were removed[30,31] and it was a better candidate for the fabrication of photo- and electro-devices. However, the deficiency of carboxylic groups at the edge of the reduced graphene oxide[32-35] was a great obstruction for the development of new photo- or electro-materials with high performance. In order to get better performance and higher grafting efficiency of hybrid materials, it is necessary to increase the density of carboxylic groups on the surface of reduced graphene oxide to graft more functionalized molecules.

In this work, a simple method was developed to obtain reduced graphene oxide with high density of carboxylic groups on its surface, in order to bond more functional groups for the fabrication of graphene hybrid. Benzoic acid functionalized with reduced graphene oxide (BFrGO) was prepared, then BFrGO was modified with symmetrically substituted zinc phthalocyanine. The obtained hybrid was well dispersed in polar solvent such as water, *N*,*N*-dimethyl formamide (DMF), dimethyl sulfoxide (DMSO) and *N*-methyl-2-pyrrolidone (NMP), of which the concentration was up to 4 mg/mL. And the wt % of 2, 9, 16, 23-tetraamino zinc phthalocyanine (ZnTAPc) in the resulting product was found to be up to 25 %. These results were attributed to the high grafting of ZnTAPc to BFrGO. The NLO properties of the hybrid was larger than that of the blend and individual samples as a result of the charge-separated excited state produced by photoinduced electron/energy transfer from the electron-donating phthalocyanine to the electron-accepting graphene.

EXPERIMENTAL

All chemical materials were of analytical grade and used without further purification unless otherwise stated. Microcrystalline graphite was purchased from Kermel Chemical Reagent Co. Ltd., Tianjin, China. *N*,*N*'-dicyclohexylcarbodiimide (DCC) and *N*-hydroxysuccinimide (NHS) was provided by Aladdin Reagent. Phthalimide and the others were obtained from Sinopharm Chemical Reagent (Beijing, China). DMF was dried by distillation over CaH_2 under reduced pressure.

FTIR spectra were recorded on a WQF-410 spectrophotometer by using KBr pellets. Raman spectra measurements were carried out with a Raman microspectroscopic setup (RamLab-010) (LabRam, Horiba-Jobin-Yvon, Bensheim, Germany) spectrometer. UV-visible spectra were taken at room temperature with a Shimadzu UV-2550 spectrophotometer. Thermal properties of the samples were measured using a HCT-1 (HENVEN, Beijing, China) comprehensive thermal analyzer in flowing (50 mL/min) nitrogen atmosphere. Fluorescence emission spectra were performed on a HITACHI 7000. The AFM samples were prepared by dropping the sample on the freshly cleaved mica and then dried naturally at room temperature at least for 24 h and measured with the instrument of NT MDT (Ntegra Prima) using a tapping mode. TEM and SEM images were recorded on a JEM-3010 and JSM-6700F microscopy, respectively. All the Z-scan experiments were used 5 ns pulses from a frequency doubled Q-switched Nd: YAG laser. The spatial profiles of the pulses were near Gaussian form after the spatial filter and focused the transmitted pulse on the sample by using 25 cm focal length lens. The laser was operated at its second harmonic, 532 nm, with a pulse repetition rate of 10 Hz. All samples were tested in 0.1 cm quartz cell.

Synthesis of ZnTAPc: The synthesis and characterization of ZnTAPc were described previously[36,37]. The synthesis and structure are shown in **Scheme-I**. ^{1}H NMR (300 MHz, DMSO-d_6): δ 8.96-8.88 (m, 4H, 4ArH), δ 8.47-8.38 (d, 4H, 4ArH), δ 7.41-7.32 (d, 4H, 4ArH), δ 6.22 (s, 8H, broad, $4NH_2$). FTIR (KBr, ν_{max}, cm^{-1}): ν 3285, 3170, 1606,

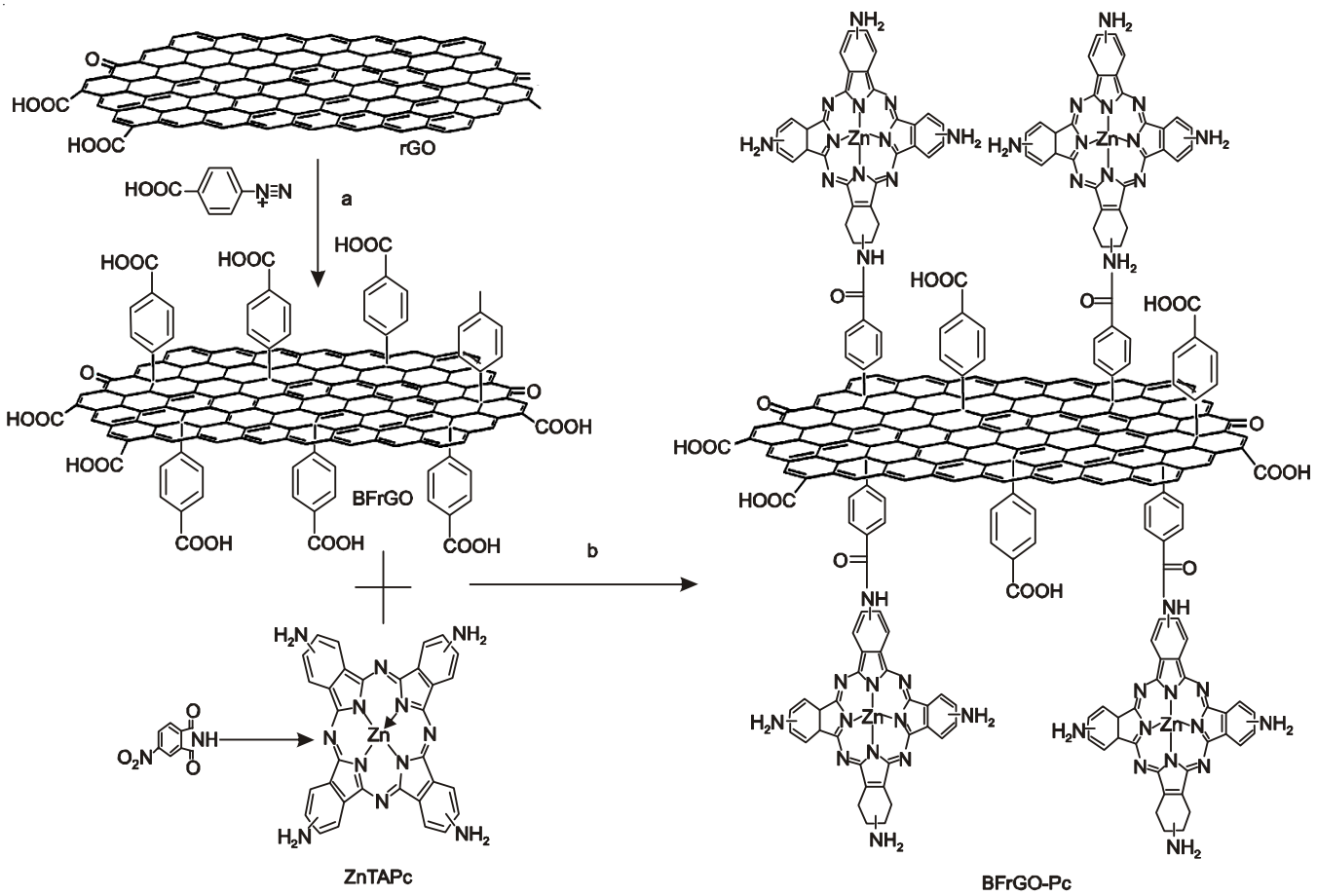

Scheme-I: Structure of ZnTAPc and preparation of ZnTAPc covalent linked with BFrGO

1490, 1402, 1342, 1305, 1249, 1134, 1091, 1043, 939, 860, 825, 736 .

Graphene oxide: Graphene oxide was prepared using a modification of Hummer's and Offeman's method from graphite powder[38-40].

Reduction of graphene oxide: The chemical reactions transforming graphene oxide into reduced graphene oxide were carried out according to the reported method[41,42]. In a typical experiment, 100 mL (1 mg/mL) of graphene oxide homogeneous dispersion (DMF) was mixed with 0.2 mL of hydrazine solution (35 wt % in water) and 1.4 mL of ammonia solution (28 wt % in water) in a 150 mL bottle. After being vigorously stirring for 5 min, the mixed solution was put in an oil bath at 95 °C under stirring for 3 h. After that, the product was filtered through a 0.2 μm PTFE membrane (micropore size 0.2 μm) and washed with water for several times, the final product was dispersed in 100 mL of water again.

Benzoic acid functionalized with reduced graphene oxide (BFrGO)[41]: Surfactant-wrapped reduced graphene oxide[43] was performed by addition of 1 g of sodium dodecylbenzen sulfonate (SDBS) to 100 mL (1 mg/mL) of reduced graphene oxide dispersion (DMF) and then sonicated for 5 min. The diazonium salt solution was added to the surfactant-wrapped reduced graphene oxide solution in an ice bath under stirring and the mixture was maintained at 0-5 °C for around 4 h. Next, the reaction mixture was stirred at room temperature for 5 h. The resulting solution was filtered using 0.2 μm PTFE membrane and washed with water, ethanol, acetone and DMF for several times sequentially. The final product was dispersed in 100 mL of DMF.

Preparation of BFrGO-Pc: The synthesis of BFrGO-Pc is shown in **Scheme-I**. The surface-bond carboxylic groups in BFrGO reacted with the NH_2 group of ZnTAPc to fabricate BFrGO-Pc nanocomposite material. Typically, DCC (26 mg) and NHS (16 mg) were added to an anhydrous DMF dispersion of purified BFrGO (20 mL, 1 mg/mL) in a 100 mL bottle and the mixture was cooled to 0 °C in an ice bath and stirred for 4 h. Next, ZnTAPc (30 mg) was added, the reaction mixture was stirred under continuous N_2 flow at room temperature for 4 days and then filtered through PTFE membrane (0.2 μm). In order to remove free phthalocyanine, the black solid was washed with DMF, acetone, methanol and water for 3 times in sequence. The obtained greenish black BFrGO-Pc was dried in vacuum at 80 °C for 12 h. For comparison, the mixture of ZnTAPc and BFrGO (BFrGO + Pc) was also prepared.

RESULTS AND DISCUSSION

The FTIR spectra of GO, BFrGO, BFrGO-Pc and Pc were showed in Fig. 1. In the spectrum of graphene oxide, the characteristic peaks are consistent with fingerprint groups such as carboxylic species (1730 cm^{-1}), hydroxyl species (OH deformation 1400 cm^{-1}, the C-OH stretching 1230 cm^{-1}) and epoxy species (1060 cm^{-1}). The peak at 1624 cm^{-1} was the vibration of water molecules absorbed[45]. In the spectrum of BFrGO pointed to an obvious absorption band emerging at 1585 cm^{-1} was attributed to the stretch of phenyl ring C=C[43-46]. The result clearly showed that the phenyl carboxylic diazonium salt was bonded to the surface of reduced graphene oxide and the vibration of the C-O-C (epoxy group) disappeared, which indicated that the GO had been well reduced. In the spectrum of BFrGO-Pc, the peak at 1730 cm^{-1} almost disappeared and a new broad band emerged at 1650 cm^{-1} corresponding to the C=O characteristic stretching bond of the amide group[47] and the new stretching band of amide C-N peak appeared at 1270 cm^{-1}. These results clearly demonstrated that the ZnTAPc molecules had been covalently bonded to the BFrGO *via* the amide linkage.

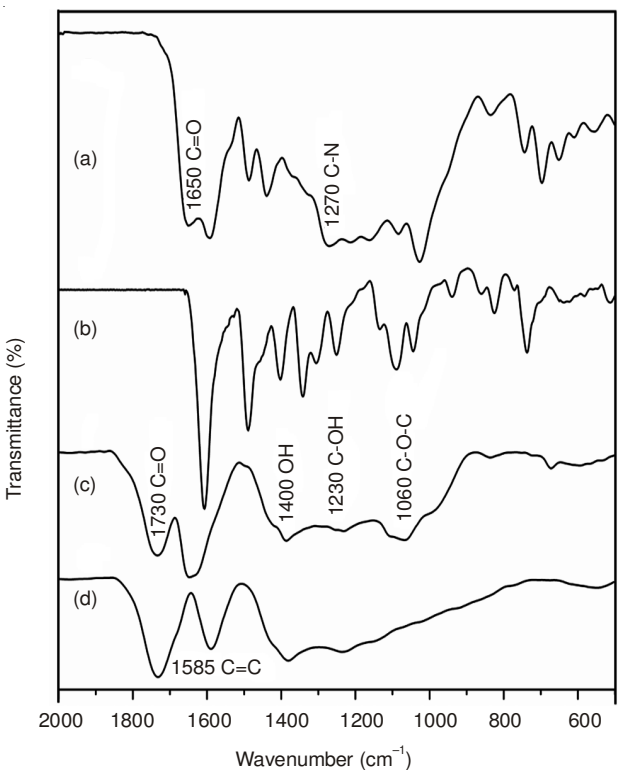

Fig. 1. FTIR spectra of (a) BFrGO-Pc, (b) Pc, (c) GO, and (d) BFrGO

Raman spectroscopy was used to explore structural characteristics of carbon materials, providing useful informations in the defects (D-band) related to the vibrations of the sp^3 hybridized carbons located at 1330 cm^{-1} and in-plane vibration of sp^2 carbon atoms (G-band) situated at 1580 cm^{-1}. The ratio of the D and G band intensities (I_D/I_G) is a useful index of the degree of functionalization[48-51]. Raman spectra of Pc, GO, reduced graphene oxide, BFrGO and BFrGO-Pc were shown in Fig. 2. In this typical set of Raman spectra, the I_D/I_G of the GO was about 1.6, after the reduced reaction the I_D/I_G decreased to 1.1. The result suggested a decrease in the disorder of the sp^2 carbon and the GO was well reduced. In the Raman spectrum of BFrGO, the intensity of D peak increased and the I_D/I_G reached to 1.2, which was attributable to the rehybridization from sp^2 to sp^3 induced by the covalent attachment of benzoic acid groups. Raman spectra results also indicated the reduced graphene oxide has been functionalized by benzoic carboxyl acid.

The morphologies of BFrGO-Pc and BFrGO hybrid material were studied by TEM, AFM and SEM (Figs. 3 and 4). Representative TEM images of BFrG-Pc material were shown in Fig. 3a, b, c. As indicated in Fig. 3a, the BFrGO-Pc

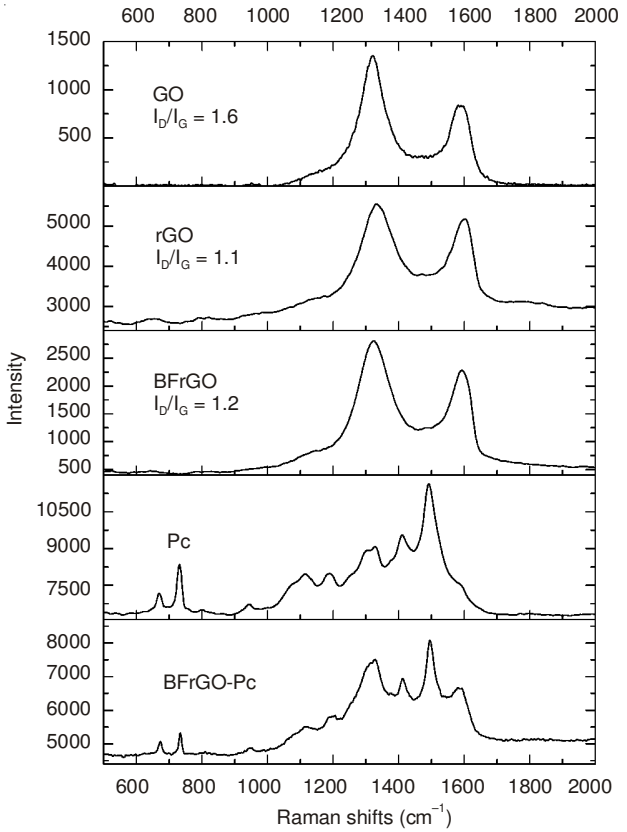

Fig. 2. Raman spectra of GO, reduced graphene oxide, BFrGO, Pc and BFrGO-Pc

was found agglomeration each other during the preparation for TEM samples. In Fig. 3b, the magnification TEM image of the encirclement area was outlined in Fig. 3a and one piece of BFrGO overlaped with the other in the image. The edge of BFrGO-Pc was roughened by the coverage of soft material significantly, indicating the presence of ZnTAPc attached to the BFrGO edge (Fig. 3b, 3c). From Fig. 3c, some periodic textures (as yellow arrows show) on the basic plane of BFrGO-Pc were observed, which could be ascribed to the one-dimensional (1D) periodic buckling structure of graphene[52]. However, the texture was discontinuous and even disappeared in some regions (as red arrows shown), which could be due to the rigid planar of ZnTAPc on graphene induced molecular flatting[53,54] and covered the ripples structure[52]. All the results demonstrated that the graphene was covered with ZnTAPc on the basic plane. Tapping mode of AFM was applied to identify the morphology of the BFrGO material. The average height of BFrGO sheets was about 1 nm, a little larger than reported apparent thickness of single-layer GO sheet (approximately 0.7 nm[41,53]) for the presence of functional phenyl carboxylic groups on the plane of the graphene (Fig. 3d). The SEM images (Fig. 4) showed that the diameter of BFrGO-Pc sheets ranged from several hundred nanometers to a few micrometers and a new greenish graphene hybrid was prepared.

The evidence for the successful functionalization of BFrGO has been supported by both Raman and FTIR spectra, TGA also agreed with the aforementioned results. As shown in Fig. 5, the onset temperature for the thermal bond cleavage

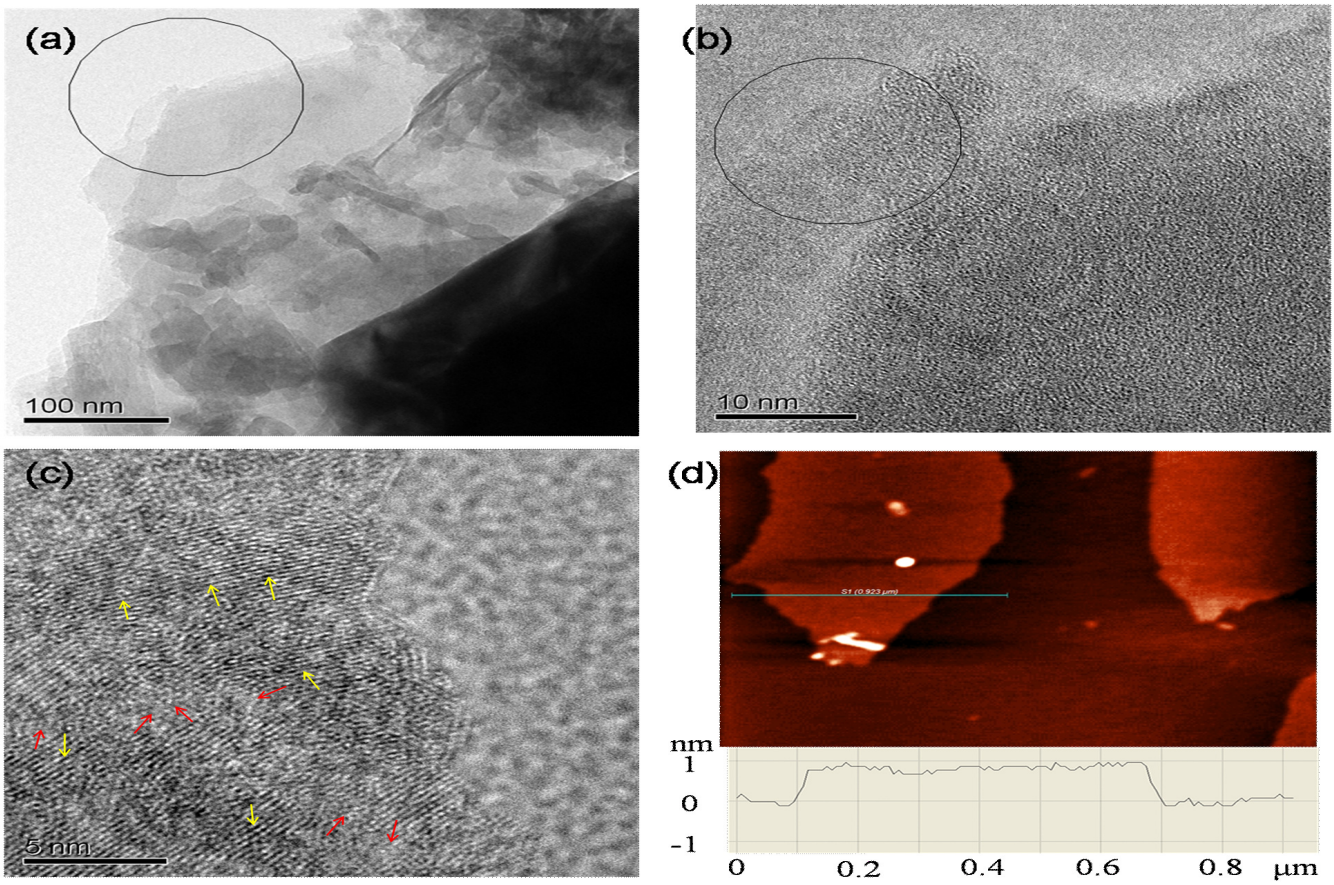

Fig. 3. (a) TEM images of BFrGO-Pc, (b) TEM image magnified and the encirclement indicated BFrGO-Pc flake, (c) HRTEM images of BFrG-Pc, (d) AFM images of BFrGO

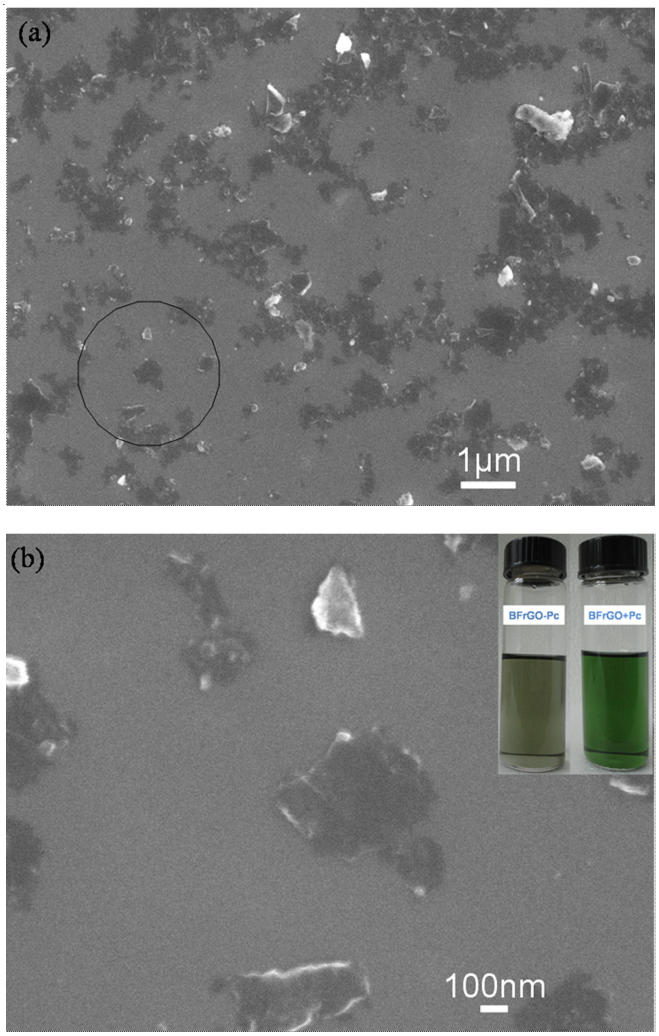

Fig. 4. (a) SEM image of BFrGO-Pc, (b) SEM image magnified. Insert image: photographs of BFrGO-Pc (13 mg/L) and BFrGO + Pc (6.5 + 6.5 mg/L)

of BFrGO and reduced graphene oxide was about 120 °C. And the weight loss between 100 and 200 °C was about 4 %, which could be due to the evaporation of organic solvents or water trapped in BFrGO. The weight loss of reduced graphene oxide, BFrGO and BFrGO-Pc between 400 and 500 °C was about 14, 19 and 21 %, which could be ascribed to the thermal cracking of the groups bond on the surface of graphene. The TGA curve of BFrGO-Pc showed a rapid weight loss of 24 % between 400 and 550 °C, followed by a slow weight loss of 10 % up to 750 °C. The weight loss for BFrGO, BFrGO-Pc and ZnTAPc was around 41, 50 and 77 % between 250 and 750 °C, respectively. Assume that the residues of ZnTAPc moiety remaining in BFrGO-Pc had the same wt % as that of ZnTAPc at 750 °C and irrespective of the wt % of water produced from the amide reaction[55]. The wt % of ZnTAPc in the resulting product could be roughly calculated and it was found to be 25 %, from which it could be clearly understood why the hybrid material was dispersed in some polar organic solvents with high concentration.

Fig. 6a showed UV-visible absorption spectra of ZnTAPc, BFrGO, BFrGO-Pc and BFrGO + Pc. ZnTAPc gave a broad Q- and B-bands around at 716 and 355 nm, while BFrGO showed strong absorption in ultraviolet range. After amide

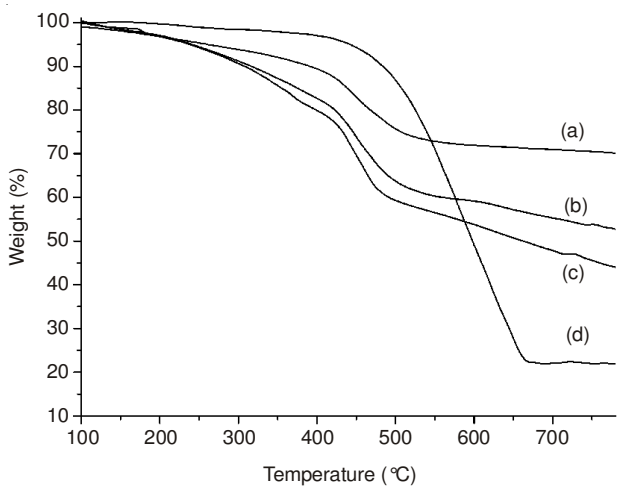

Fig. 5. TGA curves of (a) reduced graphene oxide, (b) BFrGO, (c) BFrGO-Pc and (d) ZnTAPc

reaction, the spectrum of BFrGO-Pc displayed two new maxima at 714 and 362 nm. In contrast to the case of ZnTAPc, the maxima peak of the Q- and B-bands of BFrGO-Pc shifted to the blue by $\Delta\lambda = 2$ nm and to the red by $\Delta\lambda = 6$ nm respectively, as a consequence of the electronic interactions between BFrGO and ZnTAPc (graphene was usually used as the electron acceptor, while Pc acted as the electron donor). But obvious shift was not observed for BFrGO + Pc. All these results showed that a covalent bond was formed between ZnTAPc and BFrGO. The solution dispersibility of BFrGO-Pc was investigated using UV-visible spectroscopies with different concentration as shown in Fig. 6b. A linear relationship between absorption values (714 nm) and concentrations was measured at the maximal absorption position and shown in Fig. 6c. The maximal absorption values of these solutions at the other wavelength (362 nm) were also in line with Beer's law (Fig. 6d). All of these evidence indicated the good homogeneously dispersion of BFrGO-Pc since aggregation at high concentration would cause a deviation from linearity in the Beer's plot[14,43].

The photoexcited states of ZnTAPc and BFrGO-Pc were investigated by fluorescence measurements. Fluorescence spectra of ZnTAPc, BFrGO-Pc and BFrGO + Pc were compared in Fig. 7a. Upon excitation of ZnTAPc at a Soret band of 355 nm, a typical peak appeared in the spectrum indicated that it was a strong fluorescence emission material. However, as our expected, the BFrGO+Pc exhibited 73 % quenching of the fluorescence emission, while a much stronger quenching up to 94 % was observed for BFrGO-Pc. Fig. 7b gave the fluorescence emission of BFrGO, ZnTAPc, BFrGO-Pc and BFrGO + Pc (excited at 345 nm). BFrGO showed a broad fluorescence emission spectrum around 400 to 500 nm and the peak located at 450 nm. ZnTAPc showed fluorescence emission peaks at 400 and 710 nm, while mixed with BFrGO the peak at 400 nm was shifted and the peak at 700 nm was quenching, which was attributed to the electron tansfer from ZnTAPc to BFrGO because of the π conjugation between ZnTAPc and BFrGO. In the spectrum of BFrGO-Pc, the emission peak of ZnTAPc at 380 nm was disappeared and the peak at 700 nm was quenching obviously, while the peak of BFrGO at 440 nm was increased, which demonstrated the luminescence

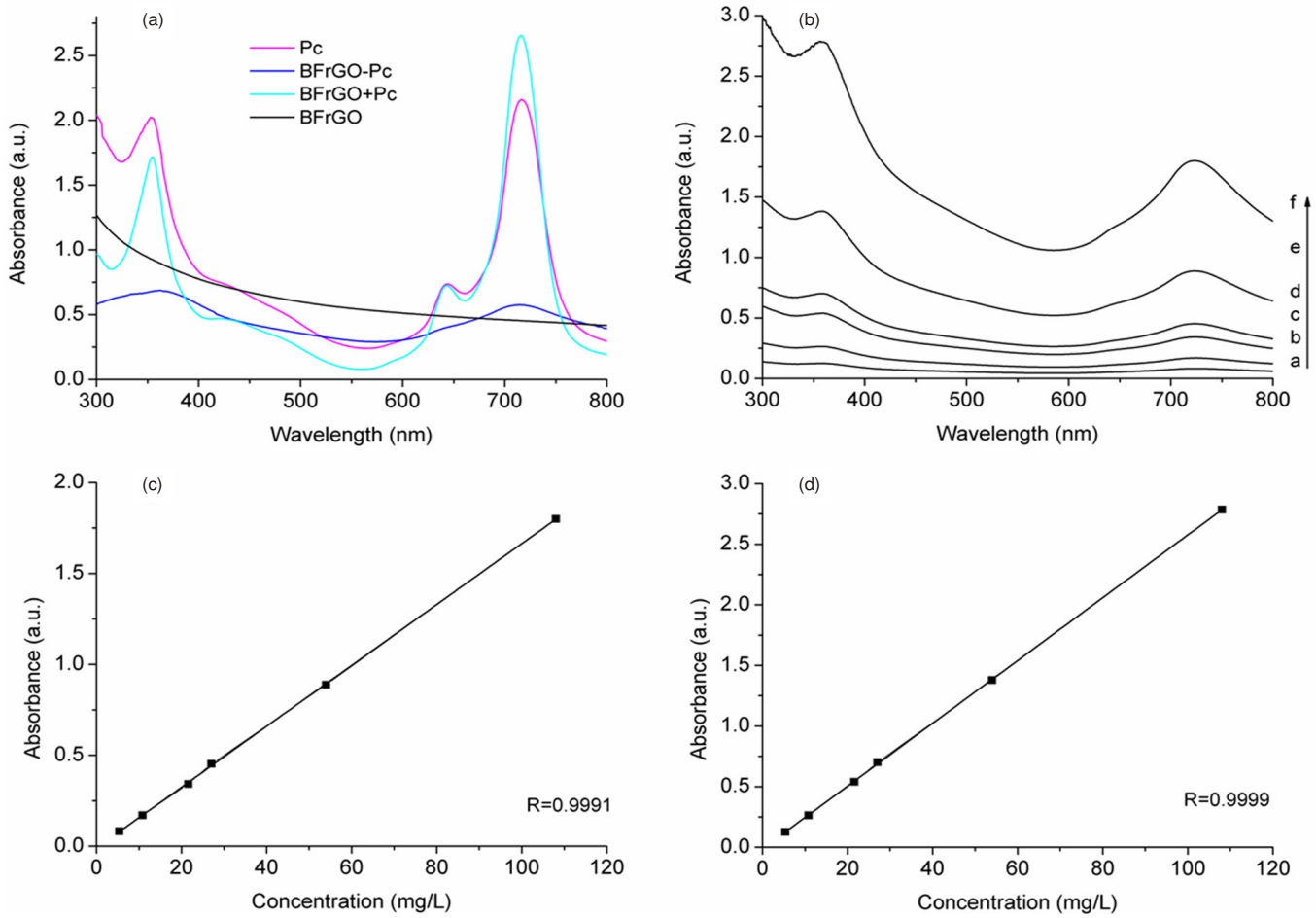

Fig. 6. (a) UV-visible absorption spectra of (BFrGO, BFrGO-Pc, ZnTAPc, and BFrGO + Pc, with the concentration of 4, 25, 13 and 6.5 + 6.5 mg/L, respectively), (b) UV-visible absorbance spectra of BFrGO-Pc (concentrations are 5.4, 10.8, 21.6, 27, 54 and 108 mg/L from a-f, respectively). The plot of optical density at 721 nm, (c) and 362 nm, (d) *vs*. concentration of BFrGO-Pc

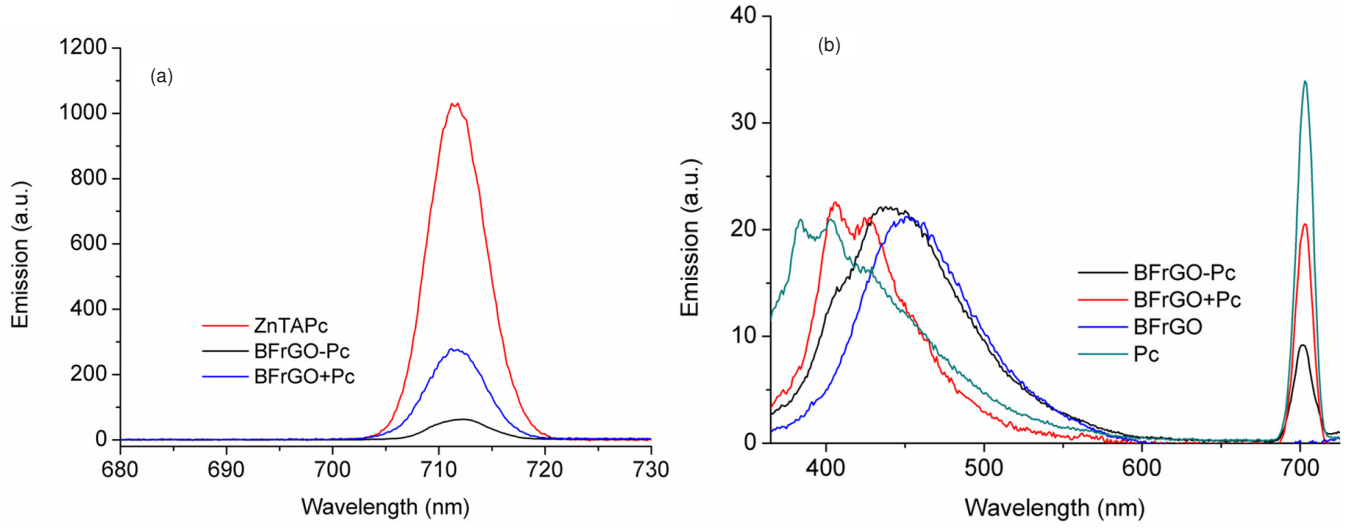

Fig. 7 Fluorescence emission spectra of (a) BFrGO-Pc and ZnTAPc in DMF (λ_{ex} = 355 nm), (b) ZnTAPc, BFrGO, BFrGO-Pc and BFrGO + Pc (λ_{ex} = 345 nm)

resonance electron tansfered from ZnTAPc to BFrGO. Possible pathways for the fluorescence quenching of the excited ZnTAPc may be attributed to two possible competitive processes: photo-induced electron transfer and energy transfer. Similar observation was also reported by other groups[17,55-57].

The open aperture Z-scan was a well-known technique to investigate the non-linear optical properties of functional materials, including nonlinear absorption, scattering and refraction[58]. The optical limiting properties of the graphene hybrid in solution were investigated using 532 nm pulsed laser irradiation and the open aperture Z-scan results of BFrGO-Pc and BFrGO + Pc were given in Fig. 8. Fig. 8a gives the open aperture Z-scan curves of BFrGO-Pc for different input fluencies. A typical limiting characteristic was observed for the results of Z-scan

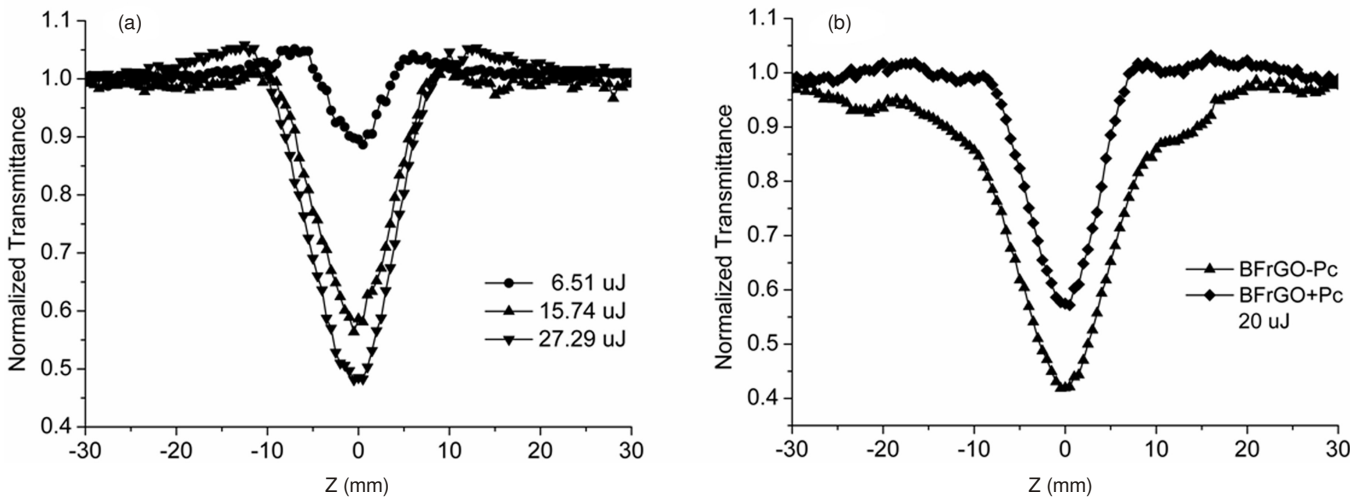

Fig. 8. (a) Typical open aperture Z-scan curves of BFrGO-Pc with the concentration of 0.161 mg/mL, (b) Open aperture Z-scan curves of BFrGO-Pc and BFrGO + Pc with the same input influence at 532 nm in the nanosecond regime with the concentration of 0.2 mg/mL

exhibited a reduction in the transmission about the focus of the lens. The normalized transmittance of curves reduced along with the increased of the on-focus intensity. The minimal normalized transmittance reached 89 % for a 0.161 mg/mL solution at the intensity of 6.51 μJ, which further decreased to 48 % as the intensity increased to 27.29 μJ. As shown in Fig. 8b the minimum transmittances at Z = 0 were 41 and 53 % for BFrGO-Pc and BFrGO + Pc, respectively. The BFrGO-Pc had the largest dip in the transmittance curves of the studied materials. Therefore, BFrGO-Pc demonstrated much better optical limiting properties comparing with the blend and individual. As well known, the Pc exhibited stronger optical limiting properties, while graphene oxide had two-photon absorption. The BFrGO-Pc was regarded as donor-bridge-acceptor and the efficient fluorescence quenching of this hybrid material could prove it. Furthermore, the possible reasons for this enhanced NLO performance may be attributed to the possible photoinduced electron and/or energy transfer mechanism between graphene and phthalocyanine.

Conclusion

A new graphene hybrid with high grafting efficiency *via* covalent bond of ZnTAPc was prepared and it was well dispersed in some polar organic solvents with high concentration. The content of ZnTAPc in the hybrid was found to be up to 25 %. In contrast to ZnTAPc, the peak maxima of the Q- and B-bands of BFrGO-Pc shifted to the blue (2 nm) and the red (6 nm), respectively, because of a consequence of the electronic interactions between ZnTAPc and graphene. The fluorescence emission of the nanohybrid was effectively quenched by a possible electron-transfer process. This material exhibited excellent NLO performance at higher intensities, which could be ascribed to the graphene counterpart.

ACKNOWLEDGEMENTS

The work was supported by the Postdoctoral Science Foundation of Central South University, Natural Science Foundation of Hunan Province (No. 11JJ3053), Key Science and Technology Financing Projects of Ministry of Education (No. 211124) of China, China Postdoctoral Science Foundation (No. 2012M521559), Scientific Research Fund of Hunan Provincial Education Department (No. 10B087) and a grant from Jishou University (No. jsdxkyzz200904), China.

REFERENCES

1. Y.M. Lin, L.A. Valdes-Garcia, S.-J. Han, D.B. Farmer, I. Meric, Y. Sun, Y. Wu, C. Dimitrakopoulos, A. Grill, P. Avouris and K.A. Jenkins, *Science*, **332**, 1294 (2011).
2. Y. Wu, Y. Lin, A.A. Bol, K.A. Jenkins, F. Xia, D.M. Farmer, Y. Zhu and P. Avouris, *Nature*, **472**, 74 (2011).
3. M. Zhou, Y.H. Lu, Y.Q. Cai, C. Zhang and Y.P. Feng, *Nanotechnology*, **22**, 385502 (2011).
4. C. Shan, H. Yang, J. Song, D. Han, A. Ivaska and L. Niu, *Anal. Chem.*, **81**, 2378 (2009).
5. D.A.C. Brownson, D.K. Kampouris and C.E. Banks, *J. Power Sources*, **196**, 4873 (2011).
6. Y. Li, J. Wang, X. Li, D. Geng, R. Li and X. Sun, *Chem. Commun.*, 9438 (2011).
7. Y. Zhu, S. Murali, M. D. Stoller. K. J. Ganesh, W. Cai, P.J. Ferreira, A. Pirkle, R.M. Wallace, K.A. Cychosz, M. Thommes, D. Su, E.A. Stach and R.S. Ruoff, *Science* **332**, 1537 (2011).
8. J.R. Miller, R.A. Outlaw and B.C. Holloway, *Science*, **329**, 1637 (2010).
9. K. Kim, J.Y. Choi, T. Kim, S.H. Cho and H.J. Chung, *Nature*, **479**, 338 (2011).
10. K.P. Loh, Q. Bao, G. Eda and M. Chhowalla, *Nat. Chem.*, **2**, 1015 (2010).
11. F. Bonaccorso, Z. Sun, T. Hasan and A.C. Ferrari, *Nat. Photonics*, **4**, 611 (2010).
12. X.F. Zhang and Q. Xi, *Carbon*, **49**, 3842 (2011).
13. N. Karousis, A.S.D. Sandanayaka, T. Hasobe, S.P. Economopoulos, E. Sarantopoulou and N. Tagmatarchis, *J. Mater. Chem.*, **21**, 109 (2010).
14. Y. Xu, Z. Liu, X. Zhang, Y. Wang, J. Tian, Y. Huang, Y. Ma, X. Zhang and Y. Chen, *Adv. Mater.*, **21**, 1275 (2009).
15. Z.B. Liu, Y.F. Xu, X.Y. Zhang, X.L. Zhang, Y.S. Chen and J.G. Tian, *J. Phys. Chem. B*, **113**, 9681 (2009).
16. S. Wang, B.M. Goh, K.K. Manga, Q. Bao, P. Yang and K.P. Loh, *ACS Nano*, **4**, 6180 (2010).
17. J. Zhu, Y. Li, Y. Chen, J. Wang, B. Zhang, J. Zhang and W.J. Blau, *Carbon*, **49**, 1900 (2011).
18. J. Wang, Y. Hernandez, M. Lotya, J. Coleman and W.J. Blau, *Adv. Mater.*, **21**, 2430 (2009).
19. Y.X. Li, J. Zhu, Y. Chen, J. Zhang, J. Wang, B. Zhang, Y. He and W.J. Blau, *Nanotechnology*, **22**, 205704 (2011).
20. J. Thompson, A. Crossley, P.D. Nellist and V. Nicolosi, *J. Mater. Chem.*, **22**, 23246 (2012).
21. M.-E. Ragoussi, J. Malig, G. Katsukis, B. Butz, E. Spiecker, G. de la Torre, T. Torres and D.M. Guldi, *Angew. Chem. Int. Ed.*, **51**, 6421 (2012).
22. X. Zhang, Y. Feng, S. Tang and W. Feng, *Carbon*, **48**, 211 (2010).

23. B. Ballesteros, G. de la Torre, C. Ehli, G.M. Aminur Rahman, F. Agulló-Rueda, D.M. Guldi and T. Torres, *J. Am. Chem. Soc*., **129**, 5061 (2007).
24. G. Bottari, G. de la Torre, D.M. Guldi and T. Torres, *Chem. Rev*., **110**, 6768 (2010).
25. X.F. Zhang, X. Cui, Q. Liu and F. Zhang, *Phys. Chem. Chem. Phys*., **11**, 3566 (2009).
26. M.E. El-Khouly, J.H. Kim, K.Y. Kay, C.S. Choi, O. Ito and S. Fukuzumi, *Chem. Eur. J.*, **15**, 5301 (2009).
27. K. Flavin, M.N. Chaur, L. Echegoyen and S. Giordani, *Org. Lett*., **12**, 840 (2010).
28. K.P. Loh, Q. Bao, P.K. Ang and J. Yang, *J. Mater. Chem.*, **20**, 2277 (2010).
29. M.J. Allen, V.C. Tung and R.B. Kaner, *Chem. Rev*., **110**, 132 (2010).
30. G. Eda, C. Mattevi, H. Yamaguchi, H. Kim and M. Chhowalla, *J. Phys. Chem. C*, **113**, 15768 (2009).
31. X. Gao, J. Jang and S. Nagase, *J. Phys. Chem. C*, **114**, 832 (2010).
32. D.W. Boukhvalov and M.I. Katsnelson, *J. Am. Chem. Soc*., **130**, 10697 (2008).
33. J.T. Paci, T. Belytschko and G.C. Schatz, *J. Phys. Chem. C*, **111**, 18099 (2007).
34. K. Erickson, R. Erni, Z. Lee, N. Alem, W. Gannett and A. Zettl, *Adv. Mater*., **22**, 4467 (2010).
35. A. Lerf, H. He, M. Forster and J. Klinowski, *J. Phys. Chem. B*, **102**, 4477 (1998).
36. B.N. Achar, G.M. Fohlen, J.A. Parker and J. Keshavayya, *Polyhedron*, **6**, 1463 (1987).
37. F.D. Cong, B. Ning, X.G. Du, C.Y. Ma, H.F. Yu and B. Chen, *Dyes Pigments*, **66**, 149 (2005).
38. L.G. Cote, F. Kim and J. Huang, *J. Am. Chem. Soc*., **131**, 1043 (2009).
39. W.S. Hummers Jr. and R.E. Offeman, *J. Am. Chem. Soc*., **80**, 1339 (1958).
40. E. Ou, X. Zhang, Z. Chen, Y. Zhan, Y. Du, G. Zhang, Y. Xiang, Y. Xiong and W. Xu, *Chem. Eur. J.*, **17**, 8789 (2011).
41. D. Li, M.B. Muller, S. Gilje, R.B. Kaner and G.G. Wallace, *Nat. Nanotechnol*., **3**, 101 (2008).
42. S. Stankovich, D.A. Dikin, R.D. Piner, K.A. Kohlhaas, A. Kleinhammes, Y. Jia, Y. Wu, S.T. Nguyen and R.S. Ruoff, *Carbon*, **45**, 1558 (2007).
43. M. Jahan, Q. Bao, J.X. Yang and K.P. Loh, *J. Am. Chem. Soc*., **132**, 14487 (2010).
44. J.R. Lomeda, C.D. Doyle, D.V. Kosynkin, W.F. Hwang and J.M. Tour, *J. Am. Chem. Soc*., **130**, 16201 (2008).
45. Y. Xu, H. Bai, G. Lu, C. Li and G. Shi, *J. Am. Chem. Soc*., **130**, 5856 (2008).
46. X. Sun, Z. Liu, K. Welsher, J.T. Robinson, A. Goodwin, S. Zaric and H. Dai, *Nano. Res*., **1**, 203 (2008).
47. S. Niyogi, E. Bekyarova, M.E. Itkis, J.L. Mcwilliams, M.A. Hamon and R.C. Haddon, *J. Am. Chem. Soc*., **128**, 7720 (2006).
48. M.M. Lucchese, F. Stavale, E.H.M. Ferreira, C. Vilani, M.V.O. Moutinho, R.B. Capaz, C.A. Achete and A. Jorio, *Carbon*, **48**, 1592 (2010).
49. A.C. Ferrari and J. Robertson, *Phys. Rev. B*, **61**, 14095 (2000).
50. S. Sarkar, E. Bekyarova, S. Niyogi and R.C. Haddon, *J. Am. Chem. Soc*., **133**, 3324 (2011).
51. R. Sharma, J.H. Baik, C.J. Perera and M.S. Strano, *Nano Lett*., **10**, 398 (2010).
52. Y. Mao, W.L. Wang, D. Wei, E. Kaxiras and J.G. Sodroski, *ACS Nano*, **5**, 1395 (2011).
53. Y. Xu, L. Zhao, H. Bai, W. Hong, C. Li and G. Shi, *J. Am. Chem. Soc*., **131**, 13490 (2009).
54. F. Schaffel, M. Wilson and J.H. Warner, *ACS Nano*, **5**, 9428 (2011).
55. N. He, Y. Chen, J. Bai, J. Wang, W.J. Blau and J. Zhu, *J. Phys. Chem. C*, **113**, 13029 (2009).
56. A. Kasry, A.A. Ardakani, G.S. Tulevski, B. Menges, M. Copel and L. Vyklicky, *J. Phys. Chem. C*, **116**, 2858 (2012).
57. X. Pan, H. Li, K.T. Nguyen, G. Gruner and Y. Zhao, *J. Phys. Chem. C*, **116**, 4175 (2012).
58. S.M. O'Flaherty, S.V. Hold, M.J. Cook, T. Torres, Y. Chen, M. Hanack and W.J. Blau, *Adv. Mater*., **15**, 19 (2003).